J. Physiol. (1987), **383**, *pp.* 93–114
With 12 *text-figures*
Printed in Great Britain

PROPERTIES OF MAINTAINED SODIUM CURRENT INDUCED BY A TOXIN FROM *ANDROCTONUS* SCORPION IN FROG NODE OF RANVIER

BY EVELYNE BENOIT AND JEAN-MARC DUBOIS

From the Laboratoire de Physiologie Comparée, bât. 443, Université Paris XI and Laboratoire de Biomembranes et des Ensembles neuronaux associé au CNRS, 91405-Orsay, France

(*Received 31 January 1986*)

SUMMARY

1. The effects of toxin II from scorpion *Androctonus australis Hector* (AaH II) on the Na current of frog myelinated nerve fibres were analysed under voltage-clamp conditions.

2. Like other α-scorpion toxins and *Anemonia* toxin II, AaH II both increased the inactivation time constants of peak Na current and induced a non-inactivatable Na current (maintained current).

3. In the presence of AaH II, the slope of the maintained conductance–voltage curve was less steep than that corresponding to the peak conductance and the maintained current reversed at a voltage about 20 mV more negative than the peak current.

4. When the peak current was inactivated by pre-depolarizations, 'on' and 'off' relaxation kinetics of the maintained current were an exponential function whose time constant changed with voltage in a bell-shaped manner. At 0 mV, the time constant was about 10 ms.

5. The effects of AaH II could be decomposed into fast effects (increase in inactivation time constants of the peak current) which developed within about 5 s and slow effects (increase in maintained current and changes in initial amplitudes of fast and slow phases of peak current inactivation) which developed within about 30 s.

6. These two types of AaH II effects could be completely removed by conditioning depolarizations giving rise to outward currents.

7. A model is proposed in which the binding of the toxin with its receptor is modulated by membrane potential and internal cations, the appearance of the maintained current is modulated by the environment of channels and the change in inactivation time constants is modulated by membrane potential. The maintained current would correspond to the transformation of a fraction of channels into a non-inactivatable (late) form.

INTRODUCTION

Several agents with diverse chemical structures are known to partly remove and/or slow Na current inactivation of excitable cells (see Schmidtmayer, 1985). Four

different models and interpretations have been proposed to describe the effects of these agents. (1) A reopening of a fraction of channels inactivated during a depolarization (Chandler & Meves, 1970; Ulbricht & Schmidtmayer, 1981). (2) An unmasking of pre-existant silent channels (Jacques, Fosset & Lazdunski, 1978). (3) A transformation of a fraction of inactivatable channels into non-inactivatable ones (Benoit, Corbier & Dubois, 1985). (4) Quantitative changes in rate constants of channel inactivation (Schmidtmayer, 1985; Wang & Strichartz, 1985). Taking into account that these models are conceptually different, it can be thought that a fine analysis of properties of peak and maintained Na currents may help to define more precisely which of them is the most credible. With this object, we analysed time- and voltage-dependent properties of Na current of frog myelinated nerve fibre poisoned with toxin II from scorpion *Androctonus australis Hector*. In neuroblastoma cells, this toxin has similar effects and binds to the same receptor site as toxin II from sea anemone *Anemonia sulcata* and α-toxins from scorpions of genera *Leiurus* and *Buthus* (Couraud, Rochat & Lissitzky, 1978; Couraud, Jover, Dubois & Rochat, 1982; Bazan & Bernard, 1984). In frog myelinated nerve fibre, the major effects of *Anemonia* and α-scorpion toxins are to induce a maintained (late) Na current ($I_{Na\,l}$) and to increase inactivation time constants of the peak Na current (Neumcke, Schwarz & Stämpfli, 1980; Ulbricht & Schmidtmayer, 1981; Meves, Rubly & Watt, 1982, 1984; Schmidtmayer, 1985). We show here that similar effects are induced by AaH II and we describe new properties of the maintained Na current. The results allow us to define more precisely the mode of action of inactivation gate modifiers.

METHODS

The experiments were carried out on nodes of Ranvier of isolated myelinated nerve fibres from frog *Rana esculenta*. The nodal membrane was voltage clamped using the method of Nonner (1969). All methods were as previously described (Benoit *et al.* 1985; Benoit & Dubois, 1985). The node was superfused with control Ringer solution or test solutions. The Ringer solution had the following composition (mM): NaCl, 111·5; KCl, 2·5; $CaCl_2$, 1·8; $NaHCO_3$, 2·4; tetraethylammonium, 10; pH, 7·4. The fibre ends were cut in a solution containing 113 mM-CsCl and 7 mM-NaCl. Samples of toxin II extracted from the venom of scorpion *Androctonus australis Hector* (AaH II) (Rochat, Bernard & Couraud, 1979) were kept at −18 °C and diluted, immediately preceding experiments, in Ringer solution. The temperature was 13–15 °C.

RESULTS

Voltage dependence of peak and maintained Na currents

Fig. 1*A* shows traces of Na current recorded under control conditions and in the presence of 70 nM-AaH II. Under control conditions, the current fully inactivated during depolarizations. In the presence of toxin, a fraction of current (maintained current) failed to inactivate during long-lasting depolarizations. This maintained current corresponded to about 30 % of the peak current and was not further increased by a 5-fold increase in toxin concentration. At 0 mV, the amplitude of the maintained current, relative to that of the peak current, varied from one fibre to another between 15 and 40 %. Peak and maintained currents, measured at various potentials before and during the application of 70 nM-AaH II, were plotted against voltage (Fig. 1*B*). The amplitude and the voltage dependence of the peak current were not significantly

modified by the toxin. Moreover, activation threshold voltages and voltages corresponding to maximum inward current, for peak and maintained currents, were identical but the maintained current reversed at a more negative potential than the peak current.

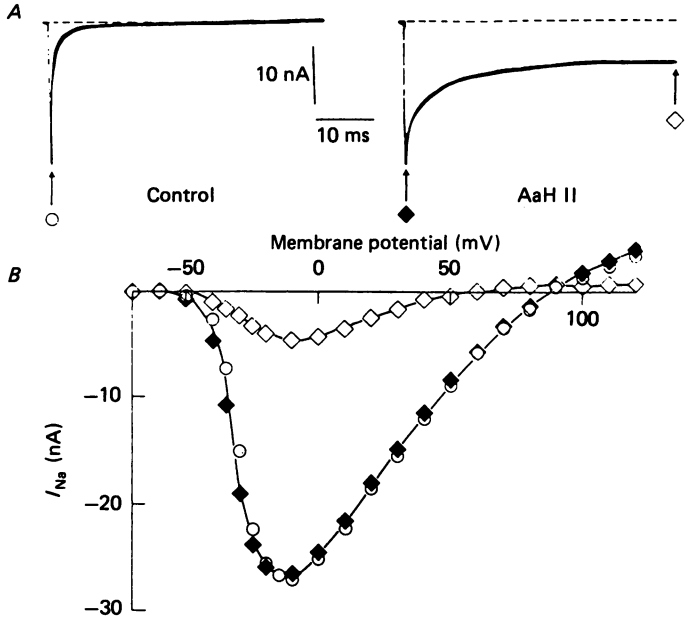

Fig. 1. Peak and AaH II-induced maintained Na current–voltage relationships. *A*, traces of Na current recorded under control conditions (left) and in the presence of 70 nM-AaH II (right) during depolarizations to 0 mV preceded by 50 ms hyperpolarizations to −120 mV. Fibre: 3-04-85. *B*, peak Na current was recorded under control conditions (open circles) and in the presence of 70 nM-AaH II (filled diamonds), and maintained Na current was recorded in the presence of 70 nM-AaH II (open diamonds) during and at the end of, respectively, 45 ms depolarizations of various amplitudes preceded by 50 ms hyperpolarizations to −120 mV. Fibre: 30-04-85.

Fig. 2 shows that, in the presence of 70 nM-AaH II, the slope of the conductance–voltage curve was less steep for maintained than for peak current. The voltage corresponding to half-maximum conductance was about 5 mV more negative for peak than for maintained current. Mean values of parameters, characterizing peak and maintained currents recorded in several fibres, are summarized in Table 1.

Reversal potentials of peak and maintained currents

The preceding results show that peak and maintained currents reversed at different potentials. In order to confirm this point, the current was recorded at various potentials in the presence of 70 nM-AaH II successively without and with 300 nM-tetrodotoxin (TTX). The current flowing through Na channels was calculated as the difference between currents recorded without and with TTX (Fig. 3). The maintained current reversed at a potential about 20 mV more negative than the reversal potential of the peak current (see also Table 1). This indicates that channels giving rise to the

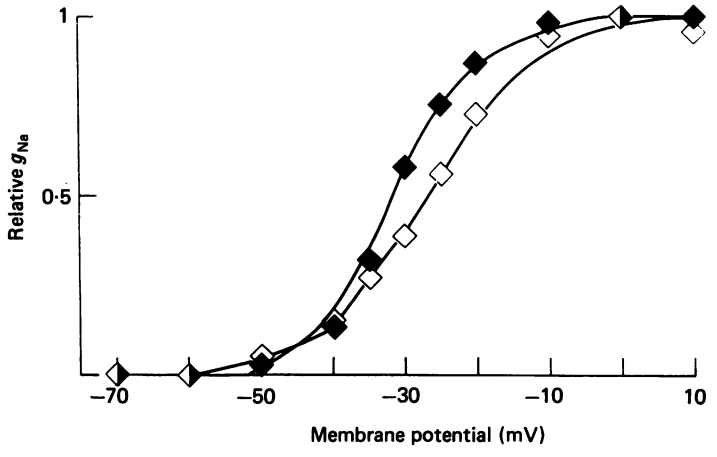

Fig. 2. Relative conductance–voltage curves as calculated from peak and maintained Na currents. Peak (filled diamonds) and maintained (open diamonds) currents were recorded in the presence of 70 nM-AaH II as described in Fig. 1*B*. Conductance values are expressed relative to the maximal conductances at large depolarizations. The curves were calculated from eqn. (1). The values of the parameters $\bar{V}$, k and a were respectively −27·5 mV, 7·5 mV and 1 (maintained) and −32 mV, 7·5 mV and 3 (peak). Fibre: 30-04-85.

TABLE 1. Characteristic parameters of maintained and peak currents in the presence of AaH II

	Maintained current	Peak current
$\bar{g}_l/\bar{g}_p$	0·38±0·03 (n = 6)	
$V_{g/2}$ (mV)	−23±2 (n = 6)	−31±3 (n = 6)
V_{th} (mV)	−45±3 (n = 6)	−45±3 (n = 6)
$V_{\bar{I}}$ (mV)	−13±2 (n = 6)	−12±2 (n = 6)
V_{rev} (mV)	+51±5 (n = 15)	+73±4 (n = 15)
$g_{\bar{V}+5}/g_{\bar{V}-5}$	1·95±0·13 (n = 6)	2·75±0·28 (n = 6)

AaH II concentration was 70 nM. $\bar{g}_l$ and $\bar{g}_p$ are the maximum maintained and peak conductances respectively. $V_{g/2}$ is the voltage corresponding to half-maximum conductance. V_{th} is the voltage corresponding to activation threshold of current. $V_{\bar{I}}$ is the voltage corresponding to maximum current. V_{rev} is the reversal potential of current. $g_{\bar{V}+5}/g_{\bar{V}-5}$ is the ratio of conductances at $V_{g/2}$±5 mV. Values are mean±S.E. of mean of n determinations.

maintained current are relatively more permeable to Cs ions than channels giving rise to the peak current. Assuming that channels corresponding to the peak current are not permeable to Cs ions (Hille, 1972), the permeability ratio P_{Cs}/P_{Na} for channels corresponding to the maintained current would be 0·078.

Relaxation kinetics of the maintained current

In Fig. 3*A*, one can observe that, when recorded near the reversal potential of the peak current, the maintained current activated relatively slowly. In order to analyse relaxation kinetics of the maintained current, the peak current was inactivated by 50 ms pre-depolarizations and the maintained current was recorded during test pulses immediately following pre-pulses (see Wang & Strichartz, 1985, Figs. 1 and 6). Fig. 4

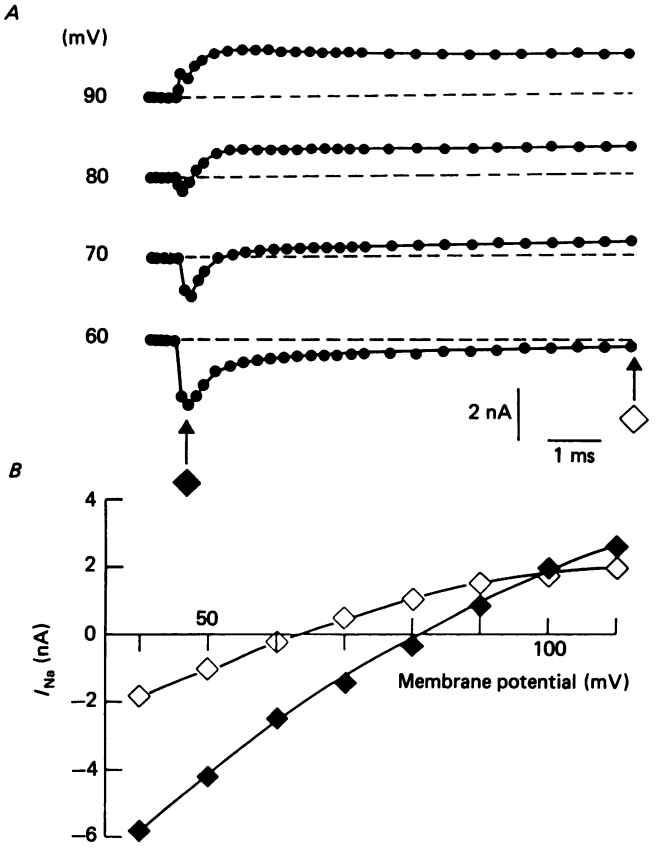

Fig. 3. Reversal potentials of peak and maintained Na currents. *A*, Na currents calculated as the difference between current traces recorded in the presence of 70 nM-AaH II, before and after addition of 300 nM-TTX, during depolarizations of various amplitudes (membrane potential given to left of trace in millivolts) preceded by 50 ms hyperpolarizations to −120 mV. *B*, peak (filled diamonds) and maintained (open diamonds) currents as a function of membrane potential. The currents were calculated as in *A*. Fibre: 6-02-85.

shows traces and semilogarithmic representations of current recorded in the presence of 70 nM-AaH II, during pulses to 0 mV preceded by depolarizations to either −30 or +30 mV. Under both conditions, the major part of the maintained current relaxation kinetics could be described by a single exponential whose time constant was 7·8 ms (turning 'on') and 9·6 ms (turning 'off'). When recorded during test pulses to various potentials between −70 and +50 mV preceded by depolarizations to or beyond −30 mV, the relaxation kinetics of the maintained current could always be described by an exponential whose time constant changed with voltage in a bell-shaped manner (Fig. 5). However, it must be noted that, when the maintained current was recorded at a given voltage, its turning 'on' was faster than its turning 'off' (Figs. 4 and 5). This point was further examined in the experiments reported in Fig. 6 which shows the variation in relaxation time constant of the maintained current recorded at 0 mV after depolarizing pre-pulses of various amplitudes. τ_{on} (for

pre-pulses to between −40 and −10 mV) was significantly smaller than τ_{off} (for pre-pulses to between +10 and +100 mV). Several explanations can be proposed for this phenomenon (see Discussion).

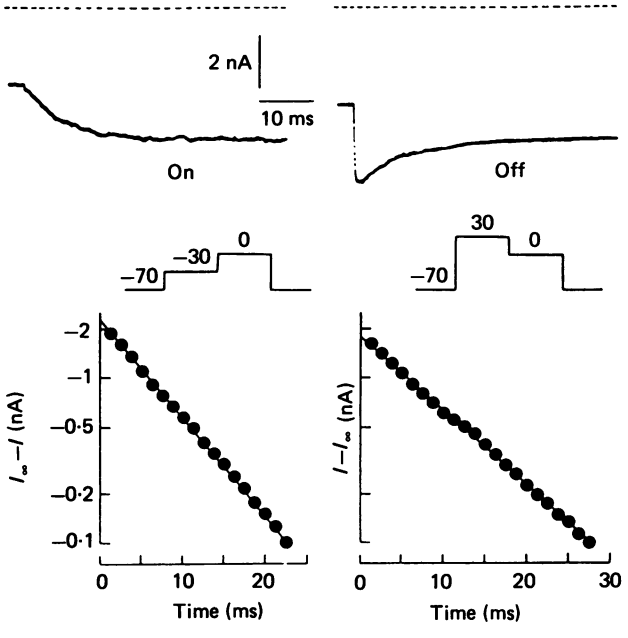

Fig. 4. 'On' and 'off' relaxation kinetics of the maintained Na current. Na current (upper traces) and representations in semilogarithmic coordinates of their relaxation kinetics (lower panels) in the presence of 70 nM-AaH II. The current was recorded during depolarizations to 0 mV preceded by 50 ms depolarizations to either −30 mV ('on') or +30 mV ('off'). Stepped traces show membrane potential (mV). The dashed lines represent zero current. The values of time constants were determined by linear-regression analysis ($r^2 \geqslant 0{\cdot}996$) using logarithms of the measured values and were 7·8 ms ('on') and 9·6 ms ('off'). I and I_∞ represent the current at times t and infinity. Fibre: 13-08-85.

Rate of action of AaH II

AaH II, like other α-scorpion toxins and *Anemonia* toxin, both induces a maintained current and alters the inactivation of the remaining peak current (see Fig. 1*A* and Introduction). In order to see whether these two types of effects were related or not, we analysed the rate of action of AaH II on the Na current by measuring the increase in maintained current and changes in time constants and initial amplitudes of inactivation phases of the peak current.

Before application of the toxin, the inactivation time course of the peak current could be described by the sum of two exponentials (Chiu, 1977; Benoit *et al.* 1985 and Fig. 7*D*). In the presence of AaH II, the maintained current should be subtracted from the total current before performing analyses of inactivation phases of the peak current. In previous works, the activation of the maintained current, induced by inactivation gate modifiers, was assumed to be faster than the inactivation of the

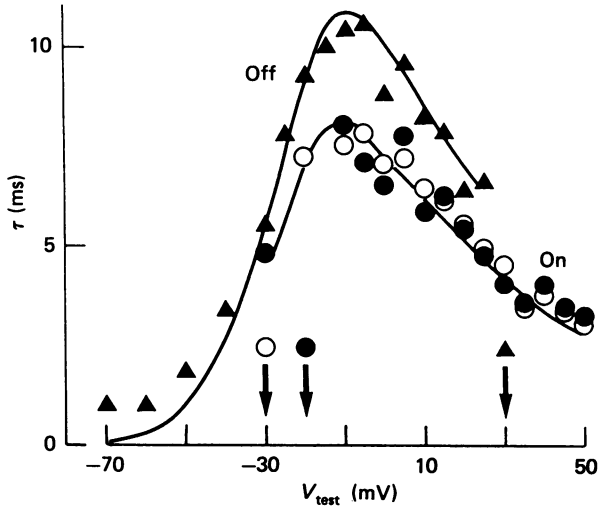

Fig. 5. Time constants of relaxation kinetics of the maintained Na current as a function of test pulse amplitude (V_{test}). The current was recorded in the presence of 70 nM-AaH II during depolarizations of various amplitudes preceded by 50 ms depolarizations to −30 mV (open circles), −20 mV (filled circles) or +30 mV (filled triangles). Time constants of relaxation kinetics (τ) were calculated as described in Fig. 4. The curves were calculated from eqn. (2). The values of the parameters $\bar{V}$, k, η and $\tau_{\bar{V}}$ were respectively −23 mV, 8 mV, 0·17 and 8·7 ms ('off') and −23 mV, 8 mV, 0·17 and 6·5 ms ('on'). Fibre: 13-08-85.

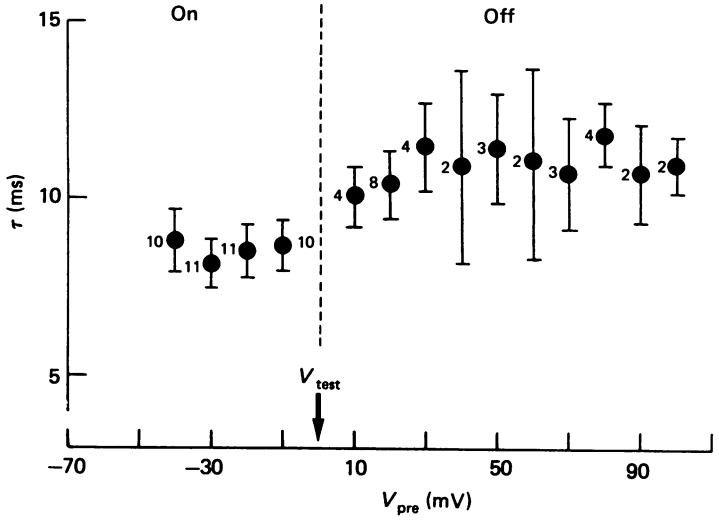

Fig. 6. Time constants of relaxation kinetics of the maintained Na current as a function of pre-pulse amplitude (V_{pre}). The current was recorded in the presence of 70 nM-AaH II during depolarizations to 0 mV preceded by 50 ms depolarizations of various amplitudes. Time constants of relaxation kinetics (τ) were calculated as described in Fig. 4. Mean values and S.E. of mean obtained in two to eleven experiments. The numbers beside each point give the number of experiments.

remaining peak current. In consequence, the maintained current, linearly extrapolated to time of depolarization, was subtracted from the total current (Bergman, Dubois, Rojas & Rathmayer, 1976; Neumcke *et al.* 1980; Ulbricht & Schmidtmayer, 1981; Meves *et al.* 1984; Schmidtmayer, 1985; Wang & Strichartz, 1985). This method was applied in Fig. 7*E* which shows that AaH II both increased fast and slow inactivation time constants and decreased the amplitude of the fast inactivation phase, extrapolated to time of depolarization. We showed above that the maintained current turned 'on' exponentially with a time constant of several milliseconds, independent of the pre-pulse amplitude (Figs. 4, 5 and 6). Consequently, it should be not linearly but exponentially extrapolated to time of depolarization. Thus, the maintained current was first recorded, as shown in Fig. 4*A*, after a pre-pulse to −30 mV. A time constant of 6 ms was calculated for its turning 'on'. Then, the maintained current was exponentially extrapolated (τ_{on} = 6 ms) to zero current at time of depolarization and subtracted from the total current (Fig. 7*C*). The semi-logarithmic representation of the inactivation of the remaining current (Fig. 7*F*) shows that it could still be described by the sum of two exponentials whose time constants and initial amplitudes were very similar to those obtained after a linear extrapolation of the maintained current. This indicates that if, in a strict sense, the linear extrapolation of the maintained current was not correct, it could be applied as a good approximation to calculate time constants and initial amplitudes of the remaining peak current inactivation. This method was applied in the experiment presented in Fig. 8. The maintained current and the time constants and initial amplitudes of the inactivation phases of the remaining peak current were calculated from traces of current recorded once per second before and during application of 70 nM-AaH II. After addition of toxin, fast and slow inactivation time constants increased and reached steady values within about 5 s. In contrast, changes in initial amplitudes of the fast inactivation phase (decrease) and the maintained current (increase) lasted about 30 s. Assuming that the amplitude of the maintained current changed exponentially, the 'on' time constant of increase in maintained current, following toxin application, was 10·6 s. The change in initial amplitude of the slow inactivation phase was more complex. After toxin application, it decreased during 3–4 s and then re-increased during about 30 s. The total current, calculated as the sum of fast and slow phases of inactivating current and maintained current amplitudes, extrapolated to time of depolarization, decreased quickly during 3–4 s and then slowly during 30 s. Similar effects of AaH II were observed on five different fibres. From these results, it appears that the effects of AaH II could be decomposed into fast effects which developed within about 5 s and slow effects which developed within about 30 s.

Removal of AaH II effects

The affinity of α-scorpion toxins for their receptor is dependent on the membrane potential (Catterall, 1979; Jover, Martin-Moutot, Couraud & Rochat, 1980; Mozhayeva, Naumov, Nosyreva & Grishin, 1980). In our experimental conditions, the fibres were held at −70 mV. If one assumes that 50 ms test depolarizations, applied at frequencies lower than 1 Hz, do not displace the toxin from its binding site, the affinity of AaH II for its receptor should be maximal (Jover *et al.* 1980;

Mozhayeva *et al.* 1980) and the effects of the toxin should be poorly reversible upon washing. This latter point was verified in the experiments presented in Fig. 9. The amplitude of the maintained current, recorded at 0 mV, was measured in different fibres before and during wash-out of 70 nM-AaH II. During wash, the decrease in maintained current amplitude could be described by an exponential whose time

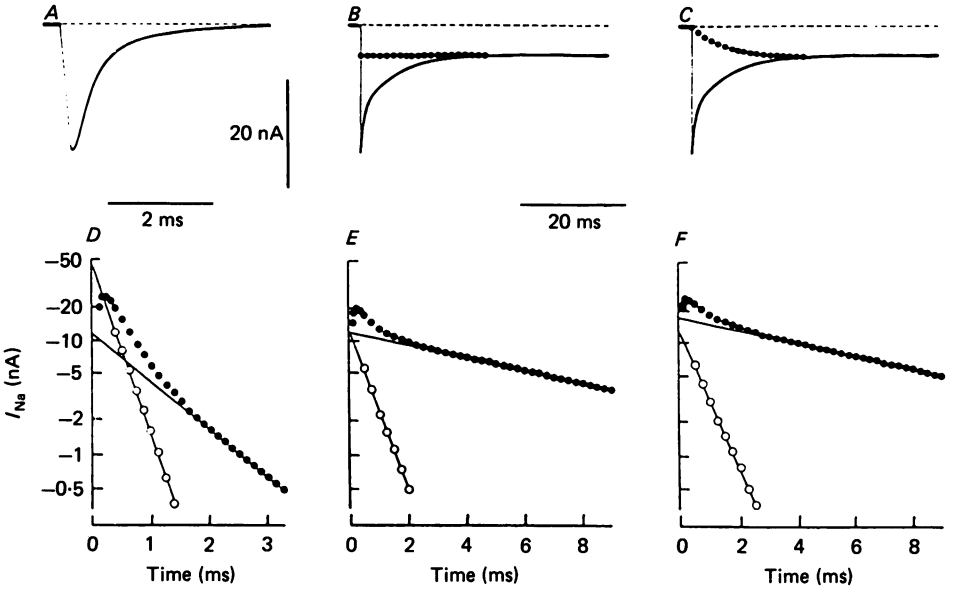

Fig. 7. Effects of AaH II on the inactivation phases of the Na current. Traces of Na current (*A*, *B* and *C*) and representations in semilogarithmic coordinates of their inactivation phases (*D*, *E* and *F*) in the absence (*A* and *D*) and presence (*B*, *C*, *E* and *F*) of 70 nM-AaH II. The current was recorded during depolarizations to 0 mV preceded by 50 ms hyperpolarizations to −120 mV. In *B* and *C*, filled circles represent the maintained current either linearly extrapolated to time of depolarization (*B*) or exponentially extrapolated (with a time constant of 6 ms) to zero current at time of depolarization (*C*). In *D*, *E* and *F*, filled circles give the over-all Na current (*D*) or over-all Na current minus the maintained current (*E* and *F*), and open circles give the fast phase of inactivation after subtraction of the slow phase of inactivation (continuous line through filled circles). The values of initial amplitudes to time of depolarization and time constants were determined by linear-regression analysis ($r^2 \geqslant 0{\cdot}996$) using logarithms of the measured values. Time constants of fast and slow phases of current inactivation were respectively 0·30 and 1·04 ms (*D*), 0·62 and 7·56 ms (*E*) and 0·72 and 7·23 ms (*F*). Initial amplitudes of fast and slow phases of current inactivation relative to their values without AaH II were respectively 0·28 and 1·19 (*E*) and 0·28 and 1·51 (*F*). Fibre: 13-08-85.

constant (τ_{off}) was 32 min (Fig. 9*A*). From this value and that of τ_{on} (Fig. 8), rate constants of binding and unbinding of the toxin could be calculated. They were $1{\cdot}34 \times 10^6$ M^{-1} s^{-1} and $0{\cdot}52 \times 10^{-3}$ s^{-1}, respectively, and for the apparent dissociation constant they gave a value (0·39 nM) very close to those calculated from binding experiments on different tissues (0·12–0·46 nM) (Rochat *et al.* 1979; Jover *et al.* 1980; Berwald-Netter, Martin-Moutot, Koulakoff & Couraud, 1981; Couraud *et al.* 1982).

In contrast with the maintained current which slowly decreased during wash-out of the toxin, inactivation time constants of the peak current did not change even after

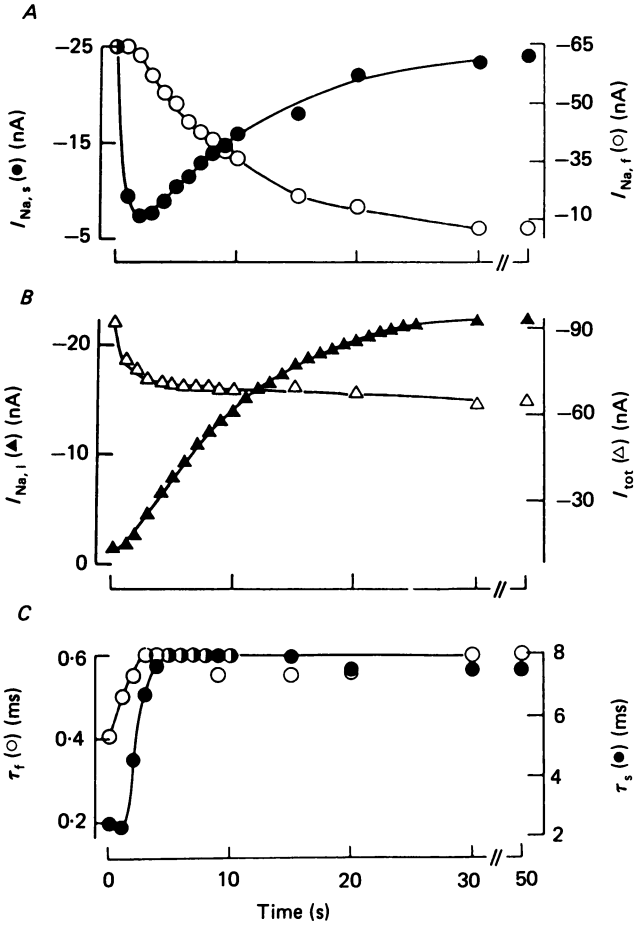

Fig. 8. Kinetics of AaH II effects on the inactivation parameters of the Na current. The current was recorded every second during depolarizations to 0 mV preceded by 50 ms hyperpolarizations to −120 mV, before and during application of 70 nM-AaH II. *A* and *B*, initial amplitudes of fast phase of inactivation ($I_{Na,f}$, open circles), slow phase of inactivation ($I_{Na,s}$, filled circles) and maintained current ($I_{Na,l}$, filled triangles), up to time of depolarization. All calculated as described in Fig. 7*B* and *E*. Total current (I_{tot}, open triangles) was calculated as the sum of initial amplitudes of fast and slow inactivation phases and maintained current. *C*, time constants of fast phase of inactivation (τ_f, open circles) and slow phase of inactivation (τ_s, filled circles), calculated as described in Fig. 7*E*. The curves were drawn by eye. Fibre: 4-01-85.

20 min of wash (Fig. 9*B*). This would suggest that, whereas the slow effects of the toxin (maintained current and changes in initial amplitudes of inactivation phases of the peak current) were reversible, the fast effects of the toxin (changes in inactivation time constants) were irreversible (but see below and Discussion).

The removal of AaH II effect on the maintained current could be accelerated by repetitive large depolarizations. In the experiment presented in Fig. 10*A*, the maintained current was partly removed by ten conditioning depolarizations to +100 mV, applied at a frequency of 0·7 Hz. The current was recorded during

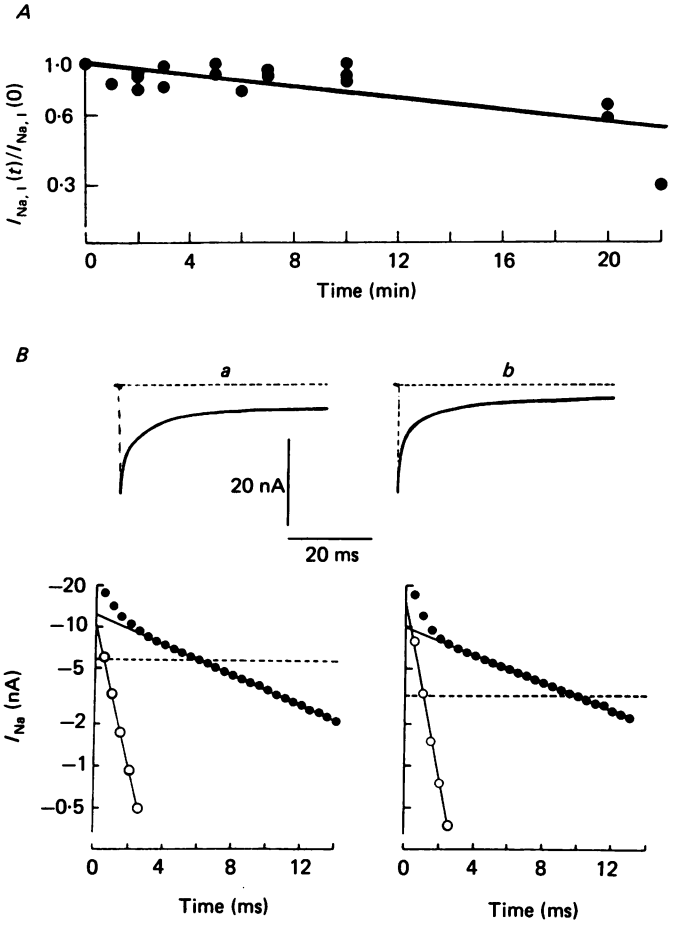

Fig. 9. Removal of AaH II effects during wash-out of the toxin. *A*, the maintained Na current was recorded in the presence and during wash-out of 70 nM-AaH II at the end of 20–90 ms depolarizations to 0 mV preceded by 50 ms hyperpolarizations to − 120 mV. The current after wash-out ($I_{Na,1}$ (*t*)) is expressed relative to its value in the presence of toxin ($I_{Na,1}$ (0)). The value of time constant of maintained current disappearance, determined by linear-regression analysis ($r^2 = 0{\cdot}55$) using logarithms of the measured values, was 32 min. Eleven experiments. *B*, traces of Na current (upper panels) and representations in semilogarithmic coordinates of their inactivation phases (lower panels) before (*a*) and after (*b*) 20 min wash-out of 70 nM-AaH II. The current was recorded during depolarizations to 0 mV preceded by 50 ms hyperpolarizations to −120 mV. The dashed lines in the lower panels represent the maintained current linearly extrapolated to time of depolarization. Filled and open circles are as described in Fig. 7*E*. Initial amplitudes of maintained current and fast and slow phases of inactivation after 20 min wash-out of AaH II, relative to their value in the presence of toxin, were respectively 0·57, 1·36 and 0·78 ($r^2 \geqslant 0{\cdot}99$). Time constants of fast and slow phases of inactivation were respectively 0·79 and 7·88 ms (*a*), and 0·66 and 8·89 ms (*b*). Fibre: 13-08-85.

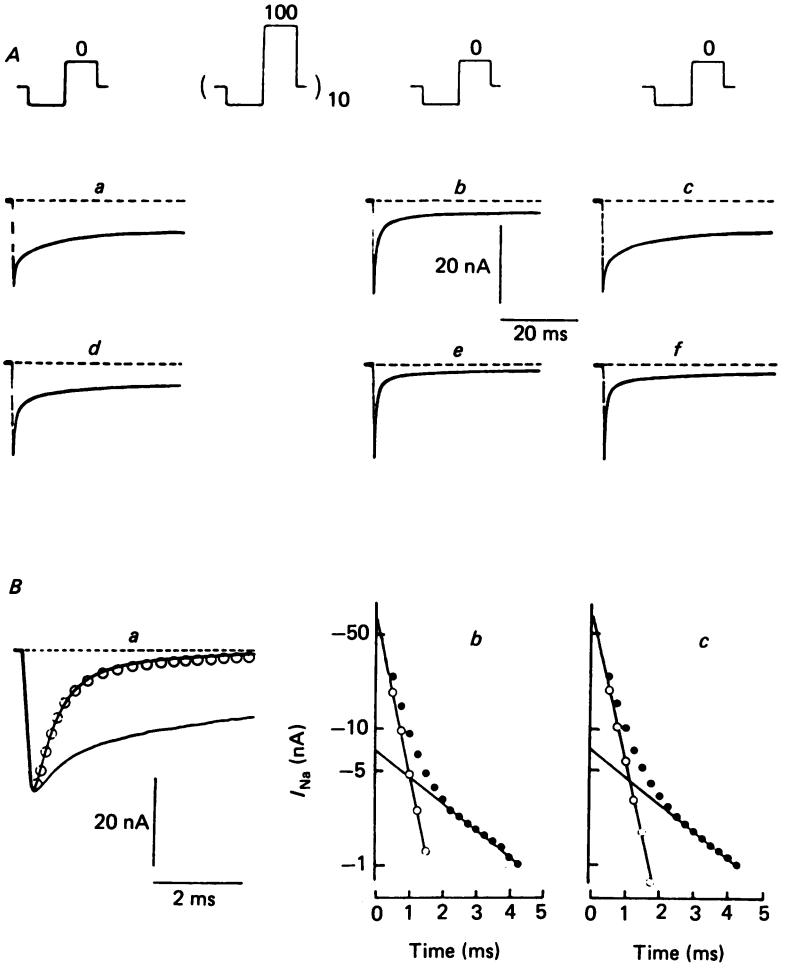

Fig. 10. Removal of AaH II effects by large conditioning depolarizations. Peak and maintained currents were recorded during depolarizations to 0 mV preceded by 50 ms hyperpolarizations to −120 mV. *A*, top trace shows membrane potential (mV); *a–f* show current recorded before (*a* and *d*), immediately after (*b* and *e*) and 2 min after (*c* and *f*) ten conditioning depolarizations (45 ms) to +100 mV, applied at a frequency of 0·7 Hz, in the presence (*a*, *b* and *c*) and 2 min after wash-out (*d*, *e* and *f*) of 70 nM-AaH II. The maintained current, which was significantly decreased just after the conditioning depolarizations, recovered after 2 min in the presence of toxin (*c*) but recovered only poorly during wash-out of the toxin (*f*). Fibre: 24-05-85. *B*, removal of AaH II effects on inactivation kinetic of the peak current. *a*, superposition of current traces before and after application of 70 nM-AaH II. Circles represent the current during wash-out of the toxin after twenty conditioning depolarizations to +100 mV. *b* and *c*, representations in semilogarithmic coordinates of peak current inactivation before application of toxin (*b*) and during wash-out of the toxin after twenty conditioning depolarizations to +100 mV (*c*). Filled and open circles are as described in Fig. 7*D*. Time constants of fast and slow phases of inactivation were respectively 0·37 and 2·25 ms (*b*) and 0·40 and 2·17 ms (*c*). Initial amplitudes of fast and slow phases of inactivation (*c*), relative to their values before toxin application, were respectively 0·96 and 1·02 ($r^2 \geqslant 0{\cdot}99$). Fibre: 23-10-85.

depolarizations to 0 mV before and after the conditioning depolarizations. 2 min after the conditioning depolarizations, the maintained current at 0 mV fully recovered in the presence of the toxin but did not in the absence of the toxin (Fig. 10*A*). During wash-out of the toxin, the two types of AaH II effects (maintained current and increased inactivation time constants) could be fully removed by twenty depolarizations to +100 mV (Fig. 10*B*). These observations, which indicate that the toxin is

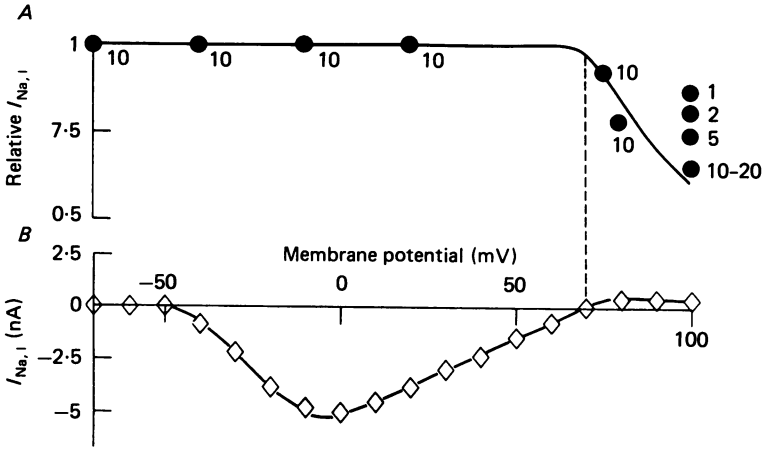

Fig. 11. Decrease in maintained current induced by conditioning depolarizations giving rise to outward currents. The maintained current was recorded in the presence of 70 nM-AaH II at the end of 49 ms depolarizations preceded by 50 ms hyperpolarizations to −120 mV. *A*, relative amplitude of maintained current as a function of voltage during conditioning depolarizations. The current was recorded at 0 mV just after 1–20 (number beside each point) conditioning depolarizations (49 ms) of various amplitudes applied at a frequency of 0·7 Hz. The amplitude of the maintained current was expressed relative to its value before conditioning depolarizations. *B*, maintained current–voltage curve. The current was recorded at the end of depolarizations of various amplitudes as described in Fig. 1*B*. Fibre: 23-10-85.

unlocked from its binding site by membrane depolarization, are in agreement with previous reported voltage dependence of α-scorpion toxin binding (Catterall, 1979; Jover *et al.* 1980; Mozhayeva *et al.* 1980; Wang & Strichartz, 1984). However, we observed that AaH II effects could only be removed by repetitive depolarizations giving rise to outward currents. This point is illustrated in Fig. 11 which shows both the change in the relative amplitude of the maintained current with the amplitude of conditioning depolarizations and the maintained current–voltage curve. The amplitude of the maintained current was not modified by ten conditioning depolarizations to below the reversal potential of the maintained current but was increasingly decreased by conditioning depolarizations to beyond the reversal potential of the maintained current as the amplitude and number of conditioning depolarizations were increased.

The preceding result suggests the existence of an interaction between the toxin binding sites and outward-going ions either within the channels or at the external face of the membrane. In this latter case, outward current would give rise to an

external accumulation of Na or Cs ions (Dubois & Coulombe, 1984). In order to test these hypotheses, three complementary experiments were undertaken. First, peak and maintained currents were recorded at 0 mV after ten conditioning depolarizations of various amplitudes in media containing 50, 100 or 150 % NaCl. The osmotic pressure was maintained at a constant level and equivalent to 150 % NaCl by sucrose. The results are presented in Fig. 12*A* which confirm that only conditioning depolarizations to beyond the reversal potential of the maintained current could displace the toxin. Moreover, we observed that the maximum maintained conductance, relative to the maximum peak conductance, was independent of the external Na concentration. Secondly, peak and maintained currents were recorded in Ringer solution containing either 100 % NaCl or 50 % NaCl + 50 % CsCl with the fibre ends cut in a solution containing 120 mM-KCl. In these conditions, the maximum maintained conductance, relative to the maximum peak conductance, was not altered either by the presence of Cs ions in the external solution or by the replacement of internal Cs by K ions. Thirdly, we observed that, at constant driving force, conditioning depolarizations were increasingly effective at displacing the toxin as the external Na concentration was increased (see Fig. 12*A*). Since the maximum Na conductance is a function of the external Na concentration (Dubois & Bergman, 1971; Landowne & Scruggs, 1981; Yamamoto, Yeh & Narahashi, 1985), this could indicate that the displacement of the toxin not only depends on the driving force but also on the conductance with the toxin being displaced by outward-going ions and outward current being increased with the maximum conductance. However, in the different media used, we observed that the outward maintained current was very small and almost independent of the external Na concentration and voltage (see Figs. 1 and 11). These observations led us to assume that (1) the displacement of the toxin was dependent on the interaction between internal cations and a channel site only accessible when the channel is open and (2) the mean open time of channels was proportional to the maximum conductance and dependent on the external Na concentration. In order to test this possibility, we plotted the variation in relative amplitude of the maintained current which was recorded at 0 mV after ten conditioning depolarizations of various amplitudes against the relative maximum maintained conductance multiplied by the driving force for the maintained current during the conditioning depolarizations. The maximum conductance was calculated between 0 and +50 mV and then expressed relative to the maximum conductance recorded in 100 % NaCl (Fig. 12*B*). Fig. 12 includes experiments made on different fibres in normal Na Ringer solution, the experiment presented in Fig. 12*A* and two experiments made either in 100 % NaCl or in 50 % NaCl + 50 % CsCl with the fibre ends cut in a solution containing 120 mM-KCl. The results confirm that the maintained current could only be decreased by conditioning depolarizations to beyond the reversal potential of the maintained current. Moreover, the decrease in maintained current, induced by conditioning depolarizations, was proportional both to the maximum maintained conductance and to the driving force for the maintained current. This strongly suggests that the toxin was displaced from its binding site by the occupancy of a site located within the channel and only accessible to internal ions (see Discussion).

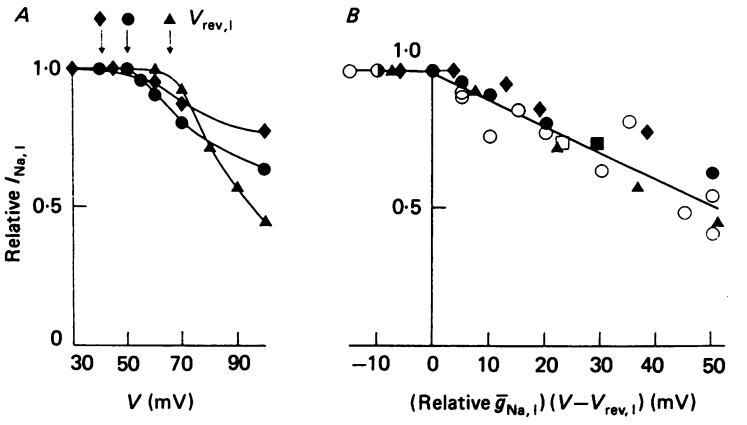

Fig. 12. Relation between amplitudes of maintained current, driving force during conditioning pulses and maximum conductance. The maintained current was recorded in the presence of 70 nM-AaH II at the end of test depolarizations (45 ms) to 0 mV preceded by 50 ms hyperpolarizations to −120 mV before and just after ten conditioning depolarizations (45 ms) of various amplitudes (see Fig. 10*A*). The amplitude of the current was expressed relative to its value before conditioning depolarizations. *A*, relative amplitude of maintained current at the end of test depolarizations as a function of voltage (*V*) during conditioning depolarizations in external media containing 50% NaCl + 100% sucrose (filled diamonds), 100% NaCl + 50% sucrose (filled circles) or 150% NaCl (filled triangles). Arrows indicate reversal potential of maintained current ($V_{rev,I}$) in each medium. The curves were drawn by eye. Fibre: 23-10-85. *B*, relative amplitude of maintained current at the end of test depolarizations as a function of the occupancy of a channel site by internal cations during conditioning depolarizations. Same experiment as in *A* plus experiments made on five other fibres in normal Na Ringer solution (open circles), in normal Na Ringer solution (filled squares) or in 50% NaCl + 50% CsCl Ringer solution (open squares) with the fibre ends cut in a solution containing 120 mM-KCl. The occupancy of channel sites during conditioning depolarizations is expressed as the maximum maintained conductance ($\bar{g}_{Na,I}$) relative to its value in 100% NaCl multiplied by the driving force for the maintained current. The curve was drawn by linear-regression analysis ($r^2 = 0{\cdot}82$).

DISCUSSION

The major findings in this paper can be summarized as follows. (1) Peak Na current and AaH II-induced maintained Na current have different voltage dependencies of activation, different reversal potentials and different activation kinetics. (2) The effects of AaH II on the Na current can be separated into fast effects (changes in inactivation time constants) and slow effects (induction of a maintained current and changes in initial amplitudes of inactivation phases of the peak current). (3) The effects of AaH II are antagonized by large depolarizations giving rise to outward currents.

Transformation of Na channels

As mentioned in the Introduction, four different models can be proposed to explain the effects of Na inactivation gate modifiers: (1) a reopening of a fraction of

inactivated channels; (2) an unmasking of pre-existent silent channels; (3) a transformation of a fraction of inactivatable channels into non-inactivatable ones and (4) quantitative changes in rate constants of channel inactivation.

According to the model proposed by Schmidtmayer (1985), consisting of quantitative changes in rate constants of inactivation, channels would have only one open state and, consequently, peak and maintained currents should reverse at the same voltage. The observation that peak and maintained currents reverse at different potentials (Figs. 1 and 3; Table 1) indicates that this model cannot explain all the effects of the toxin.

It must be noted that, in contrast with the maintained current induced by toxin II from scorpion *Androctonus australis Hector*, the maintained current induced by toxin II from scorpion *Leiurus quinquestriatus* reverses at the same voltage as the peak current (Wang & Strichartz, 1985). This indicates that the properties of Na channels are differentially modified by various α-scorpion toxins.

Any of the other models proposed cannot be definitively rejected on the basis of the present observations. However, the observation that, following toxin treatment, the initial amplitudes of fast and slow inactivation phases and maintained current change simultaneously (Fig. 8) is in favour of the interconversion hypothesis that we recently proposed (Benoit *et al.* 1985) which consists of a transformation of fast channels into slow and late channels. The fast and slow channels corresponded to fast and slow inactivation phases of the peak current, respectively. The effects of AaH II on the global Na current can be explained if one assumes that, while the toxin binds to a single class of receptors (Jover *et al.* 1980; Wang & Strichartz, 1985), it exerts two separate types of actions on Na channels. First, it induces an increase in inactivation time constants (Figs. 7 and 8). Then, it would induce a transformation of fast (F) channels into slow (S) and late (L) channels according to the scheme:

$$\mathrm{F} \rightleftharpoons \mathrm{S} \rightleftharpoons \mathrm{L}, \qquad (A)$$

where the late channels would give rise to the slowly activating maintained current.

The two types of effects of AaH II can be explained on the basis of a model already proposed by Schmidtmayer, Stoye-Herzog & Ulbricht (1982) to describe the delayed appearance of the maintained current induced by *Anemonia* toxin (see also Fig. 8*B*). This model consists of two consecutive reactions:

$$\mathrm{R}+\mathrm{T} \rightleftharpoons \mathrm{RT} \rightleftharpoons \mathrm{R^*T}, \qquad (B)$$

where a toxin molecule (T) binds to a receptor (R) to form a first complex (RT), which is then transformed into R*T. According to this model, the first reaction occurs within 5 s after the addition of the toxin and induces changes in inactivation rate constants. The second reaction corresponds to the transformation of channels according to scheme (*A*). In the presence of a saturation concentration of toxin, all channels are modified (RT) but, because of the reversibility of the second reaction, only a fraction of channels is transformed into late channels. From a molecular point of view, this can be explained if one assumes that, in the presence of toxin, the emergence of late channels is, in some ways, controlled by the environment of channels and only about 30 % of channels have an environment favourable to their transformation into the late form. This interpretation is supported by the observation that α-scorpion toxins do not induce maintained current in neuroblastoma cells (Gonoi, Hille & Catterall,

1984; Bazan & Bernard, 1984) whose membrane lipid properties are assumed to be different from those of non-malignant cells (De Laat, Van Der Saag & Shinitzky, 1977).

The reduction of total current (Fig. 8) induced by AaH II can be due to a loss of a fraction of channels (Schmidtmayer, 1985) and/or a smaller unitary conductance of late or slow channels than for fast channels (Conti, Hille, Neumcke, Nonner & Stämpfli, 1976).

Kinetics and voltage dependence of the maintained current

The observation that the turning 'on' of the maintained current can be described by a single exponential (Fig. 4) suggests that the opening of late channels follows a single two-state transition between closed and open configurations. In other words, the opening of late channels is controlled by only one activation gate.

According to the physical interpretation of the Hodgkin–Huxley model (Hodgkin & Huxley, 1952), the peak conductance–voltage curve can be described by the Boltzman equation (Keynes & Rojas, 1974):

$$g_{Na} = \bar{g}_{Na}\left(\frac{1}{1+\exp\left[(\overline{V}-V)/k\right]}\right)^{a}, \tag{1}$$

where g_{Na} is the Na conductance, $\bar{g}_{Na}$ is the maximum Na conductance, V is the membrane potential, $\overline{V}$ is the potential at which gating charges are equally distributed between closed and open configurations, k is the steepness factor including the effective valency of gates and a is the number of activation gates per channel. Following the above considerations, the exponent a would equal 1 for the maintained conductance whereas it equals 2 or 3 for the peak conductance (Frankenhaeuser, 1960; Dodge, 1963; Neumcke, Nonner & Stämpfli, 1976).

The results presented in Fig. 2 support this hypothesis. In Fig. 2, the curves were calculated from eqn. (1) with a equal to 3 and 1 for peak and maintained conductances, respectively. The value of k was identical (7·5 mV) for both curves and $\overline{V}$ was 4·5 mV more positive for maintained than for peak conductance. Although, if one considers both charge movement and conductance, eqn. (1) is inadequate to describe the voltage dependence of normal channels (see Neumcke *et al.* 1976), the present results show that it can be used to describe the effects of AaH II if one assumes that the toxin immobilizes, in an open configuration, two out of three gates per channel transformed into the late form. This would result in a decrease in maximum charge movement and is in agreement with results obtained with *Leiurus* scorpion venom (Nonner, 1979) and *Anemonia* toxin (Neumcke, Schwarz & Stämpfli, 1985).

Assuming a single energy barrier located between two possible sites that the gating particles can occupy, the time constant–voltage relationships shown in Fig. 5 can be described by the equation:

$$\tau = \frac{2\tau_{\overline{V}}}{\exp\left[(\overline{V}-V)(1-\eta)/k\right]+\exp\left[(V-\overline{V})\eta/k\right]}, \tag{2}$$

(Adrian, 1978; Horowicz & Schneider, 1981; Dubois & Schneider, 1982, 1985) where V, $\overline{V}$ and k are the same parameters as in eqn. (1), $\tau_{\overline{V}}$ is the value of τ at $\overline{V}$ and η is the fraction of the total field between sites that appears between the barrier and

the resting site. The data points in Fig. 5 are well fitted by eqn. (2) with values of $\overline{V}$ and k very similar to those calculated from the conductance–voltage curve. The value of η used (0·17) was significantly smaller than the values found in the same preparation for normal charge movement (0·50–0·69) or batrachotoxin-modified Na current and charge movement (0·77) (Dubois & Schneider, 1982, 1985). This indicates that AaH II would displace the potential barrier seen by the gating particles of late channels.

A remaining unexplained point is that, at the same voltage, τ_{off} of the maintained current is larger than τ_{on} (Figs. 5 and 6). In the node of Ranvier, differences between τ_{on} and τ_{off} have been reported for normal charge movement (Dubois & Schneider, 1982). However, in this case, in contrast with the present observation τ_{off} was smaller than τ_{on}. For the AaH II-induced maintained current, the difference between τ_{on} and τ_{off} can be due either to time- and voltage-dependent changes in apparent rate constants for channel transition between closed and open states (Dubois & Schneider, 1982) or accumulation–depletion of Na ions near the membrane (Dubois & Coulombe, 1984). For 'off' relaxation analyses, the membrane was pre-depolarized to potentials at which the maintained current was relatively small and thus should not induce noticeable changes in Na concentrations near the membrane. In contrast, for 'on' relaxation analyses, the membrane was pre-depolarized to potentials giving rise to relatively large inward maintained currents which should induce a depletion of Na ions into the nodal gap. Consequently, the external Na concentration could differentially change during 'on' and 'off' maintained current relaxations and could differentially alter the apparent 'on' and 'off' time constants. Experiments in which Na depletion is reduced would help to define more precisely the origin of the difference between 'on' and 'off' time constants.

Interaction between internal ions and AaH II

The results presented in Figs. 10, 11 and 12 show that the toxin can be removed from its binding site by large depolarizations giving rise to outward currents. However, it is clear from Figs. 11 and 12 that the displacement of the toxin from its binding site is not directly dependent on the outward current but is instead dependent on the driving force and maximum conductance. One interpretation of these results is to assume that the occupancy by internal cations of a site located within the channel decreases the affinity of the channel for the toxin. This occupancy would depend on voltage and accessibility of the site. Assuming that the increase in maximum conductance in high Na solution is, at least partly, due to an increase in the mean open time of channels (see Swenson & Armstrong, 1981), the results suggest that the binding of internal cations to the channel site would occur only when the activation gate is open and that these internal cations would be knocked off their binding sites by in-going ions. This conclusion is very similar to that drawn for the blocking of the K channels by internal cations (Armstrong & Hille, 1972; Hille & Schwartz, 1978).

Although this hypothesis should be confirmed by further experiments, it can help to explain discrepancies in voltage dependence of α-scorpion toxin binding reported by Catterall (1979) on one hand and by Mozhayeva *et al.* (1980) on the other hand. Mozhayeva *et al.* analysed the voltage dependence of toxin binding under voltage-

clamp conditions and found a relation between toxin affinity and inactivation of Na channels. Under these experimental conditions, since the membrane was held at various negative voltages, the driving force for permeant ions was always negative and the change in apparent toxin affinity must reflect a pure voltage dependence of the toxin binding or a direct effect of electric field on the positively charged toxin molecules (Woodhull, 1973; Mozhayeva *et al.* 1980). On the contrary, Catterall (1979) depolarized the membrane by replacing Na by K ions in the external solution and found a relation between toxin binding and activation of Na channels. Under these experimental conditions, the change in toxin affinity could, at least in part, be due to the change in driving force and activation of Na channels.

A remaining point is to explain why the effects of the toxin on the maintained current were reversible whereas the effects of the toxin on the inactivation time constants of the peak current were irreversible when the membrane was stimulated by moderate depolarizations, but were reversible when the membrane was stimulated by large depolarizations (Figs. 9 and 10). A hypothetical explanation is that the two types of effects of the toxin are dependent not only on toxin binding but also on other factors. The appearance of the maintained current could be dependent on the environment of the channel (see above) and the change in inactivation time constants could be dependent on membrane voltage (cf. Meves *et al.* 1984) according to the scheme:

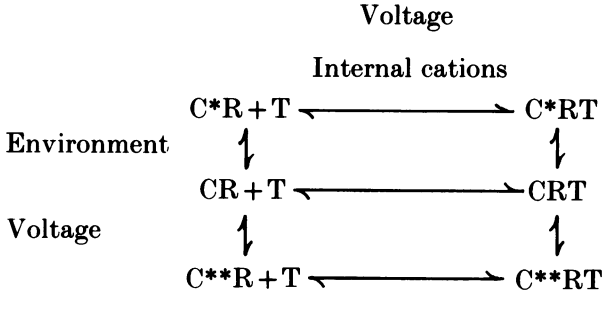

(*C*)

where R represents the toxin receptor associated with the channel (C). The affinity of the receptor for the toxin is decreased by membrane depolarization and interaction of internal cations with a channel site. The appearance of late channels (C*RT), corresponding to the maintained current, is dependent on the environment of channels, and the increase in inactivation time constants (C**RT) is dependent on voltage. On the basis of this hypothesis, the results can be explained if one assumes that during wash-out of the toxin, the transition C* ⟷ C is reversible whereas the transition C** ⟷ C can only be reversed by depolarizations. Moreover, in the absence of toxin, the transitions C ⟷ C* and C ⟷ C** could occur either after incorporation within the membrane of various inactivation gate modifiers (see Schmidtmayer, 1985) or in normal conditions (Dubois & Bergman, 1975; Meves *et al.* 1984).

If scheme (*C*) can explain the effects of AaH II on the Na current of frog node of Ranvier, it raises questions which need further experiments to be answered. For instance, the apparent dissociation constant calculated from the appearance of the

maintained current (see Results) should not correspond to the effective dissociation constant of the toxin binding. Moreover, scheme (*C*) could be inadequate to describe the effects of different inactivation gate modifiers on a given preparation on one hand, and the effects of a given inactivation gate modifier on various preparations on the other hand (see Wang & Strichartz, 1985). Separate alterations of the different transitions in scheme (*C*) associated with biochemical and electrophysiological studies could help to define its validity more precisely.

We thank F. Couraud and H. Rochat for a generous gift of AaH II. This work was supported by grants from the Ministère de la Recherche et de la Technologie (85 C 1134) and from the Institut National de la Santé et de la Recherche Médicale (83 6010).

REFERENCES

ADRIAN, R. H. (1978). Charge movement in the membrane of striated muscle. *Annual Review of Physiology and Bioengineering* **7**, 85–112.

ARMSTRONG, C. M. & HILLE, B. (1972). The inner quaternary ammonium ion receptor in potassium channels of the node of Ranvier. *Journal of General Physiology* **59**, 388–400.

BAZAN, M. & BERNARD, P. (1984). Effet des neurotoxines alpha de venin de scorpion sur le courant sodium des cellules de neuroblastome. *Journal de Biophysique et de Médecine Nucléaire* **8**, 3–8.

BENOIT, E., CORBIER, A. & DUBOIS, J. M. (1985). Evidence for two transient sodium currents in the frog node of Ranvier. *Journal of Physiology* **361**, 339–360.

BENOIT, E. & DUBOIS, J. M. (1985). Cooperativity of tetrodotoxin action in the frog node of Ranvier. *Pflügers Archiv* **405**, 237–243.

BERGMAN, C., DUBOIS, J. M., ROJAS, E. & RATHMAYER, W. (1976). Decreased rate of sodium inactivation in the node of Ranvier induced by a polypeptide from sea anemone. *Biochimica et biophysica acta* **455**, 173–184.

BERWALD-NETTER, Y., MARTIN-MOUTOT, N., KOULAKOFF, A. & COURAUD, F. (1981). Na^+-channel-associated scorpion toxin receptor sites as probes for neuronal evolution *in vivo* and *in vitro*. *Proceedings of the National Academy of Sciences of the U.S.A.* **78**, 1245–1249.

CATTERALL, W. A. (1979). Binding of scorpion toxin to receptor sites associated with sodium channels in frog muscle. Correlation of voltage-dependent binding with activation. *Journal of General Physiology* **74**, 375–391.

CHANDLER, W. K. & MEVES, H. (1970). Evidence for two types of sodium conductance in axons perfused with sodium fluoride solutions. *Journal of Physiology* **211**, 653–678.

CHIU, S. Y. (1977). Inactivation of sodium channels: second order kinetics in myelinated nerve. *Journal of Physiology* **273**, 573–596.

CONTI, F., HILLE, B., NEUMCKE, B., NONNER, W. & STÄMPFLI, R. (1976). Conductance of the sodium channel in myelinated nerve fibres with modified sodium inactivation. *Journal of Physiology* **262**, 729–742.

COURAUD, F., JOVER, E., DUBOIS, J. M. & ROCHAT, H. (1982). Two types of scorpion toxin receptor sites, one related to the activation, the other to the inactivation of the action potential sodium channel. *Toxicon* **20**, 9–16.

COURAUD, F., ROCHAT, H. & LISSITZKY, S. (1978). Binding of scorpion and sea anemone neurotoxins to a common site related to the action potential Na^+ ionophore in neuroblastoma cells. *Biochemical and Biophysical Research Communications* **83**, 1525–1530.

DE LAAT, S. W., VAN DER SAAG, P. T. & SHINITZKY, M. (1977). Microviscosity modulation during the cell cycle of neuroblastoma cells. *Proceedings of the National Academy of Sciences of the U.S.A.* **74**, 4458–4461.

DODGE, F. A. (1963). A study of ionic permeability changes underlying excitation in myelinated nerve fibres of the frog. Thesis. The Rockefeller University. University Microfilms, Inc. Ann. Arbor (No. 64-7333).

DUBOIS, J. M. & BERGMAN, C. (1971). Variation de la conductance sodium de la membrane nodale

en fonction de la concentration en ions Na^+. *Comptes Rendus de l'Académie des Sciences de Paris* **272**, 2796–2799.

DUBOIS, J. M, & BERGMAN, C. (1975). Late sodium current in the node of Ranvier. *Pflügers Archiv* **357**, 145–148.

DUBOIS, J. M. & COULOMBE, A. (1984). Current-dependent inactivation induced by sodium depletion in normal and batrachotoxin-treated frog node of Ranvier. *Journal of General Physiology* **84**, 25–48.

DUBOIS, J. M. & SCHNEIDER, M. F. (1982). Kinetics of intramembrane charge movement and sodium current in frog node of Ranvier. *Journal of General Physiology* **79**, 571–602.

DUBOIS, J. M. & SCHNEIDER, M. F. (1985). Kinetics of intramembrane charge movement and conductance activation of batrachotoxin-modified sodium channels in frog node of Ranvier. *Journal of General Physiology* **86**, 381–394.

FRANKENHAEUSER, B. (1960). Quantitative description of sodium currents in myelinated nerve fibres of *Xenopus laevis*. *Journal of Physiology* **151**, 491–501.

GONOI, T., HILLE, B. & CATTERALL, W. A. (1984). Voltage clamp analysis of sodium channels in normal and scorpion toxin-resistant neuroblastoma cells. *Journal of Neuroscience* **4**, 2836–2842.

HILLE, B. (1972). The permeability of the sodium channel to metal cations in myelinated nerve. *Journal of General Physiology* **59**, 637–658.

HILLE, B. & SCHWARZ, W. (1978). Potassium channels as multi-ion single file pores. *Journal of General Physiology* **72**, 409–442.

HODGKIN, A. L. & HUXLEY, A. F. (1952). A quantitative description of membrane current and its application to conduction and excitation in nerve. *Journal of Physiology* **117**, 500–544.

HOROWICZ, P. & SCHNEIDER, M. F. (1981). Membrane charge moved at contraction thresholds in skeletal muscle fibres. *Journal of Physiology* **314**, 595–633.

JACQUES, Y., FOSSET, M. & LAZDUNSKI, M. (1978). Molecular properties of the action potential Na^+ ionophore in neuroblastoma cells. *Journal of Biological Chemistry* **253**, 7383–7392.

JOVER, E., MARTIN-MOUTOT, N., COURAUD, F. & ROCHAT, H. (1980). Binding of scorpion toxins to rat brain synaptosomal fraction. Effects of membrane potential, ions, and other neurotoxins. *Biochemistry* **19**, 463–467.

KEYNES, R. D. & ROJAS, E. (1974). Kinetic and steady-state properties of the charged system controlling sodium conductance in the squid giant axon. *Journal of Physiology* **239**, 393–434.

LANDOWNE, D. & SCRUGGS, V. (1981). Effects of internal and external sodium on the sodium current–voltage relationship in the squid giant axon. *Journal of Membrane Biology* **59**, 79–89.

MEVES, H., RUBLY, N. & WATT, D. D. (1982). Effect of toxins isolated from the venom of the scorpion *Centruroides sculpturatus* on the Na currents of the node of Ranvier. *Pflügers Archiv* **393**, 56–62.

MEVES, H., RUBLY, N. & WATT, D. D. (1984). Voltage-dependent effect of a scorpion toxin on sodium current inactivation. *Pflügers Archiv* **402**, 24–33.

MOZHAYEVA, G. N., NAUMOV, A. P., NOSYREVA, E. D. & GRISHIN, E. V. (1980). Potential-dependent interaction of toxin from venom of the scorpion *Buthus eupeus* with sodium channels in myelinated fibre. Voltage clamp experiments. *Biochimica et biophysica acta* **597**, 587–602.

NEUMCKE, B., NONNER, W. & STÄMPFLI, R. (1976). Asymmetrical displacement current and its relation with the activation of sodium current in the membrane of frog myelinated nerve. *Pflügers Archiv* **363**, 193–203.

NEUMCKE, B., SCHWARZ, W. & STÄMPFLI, R. (1980). Modification of sodium inactivation in myelinated nerve by *Anemonia* toxin II and iodate. Analysis of current fluctuations and current relaxations. *Biochimica et biophysica acta* **600**, 456–466.

NEUMCKE, B., SCHWARZ, W. & STÄMPFLI, R. (1985). Comparison of the effects of *Anemonia* toxin II on sodium and gating currents in frog myelinated nerve. *Biochimica et biophysica acta* **814**, 111–119.

NONNER, W. (1969). A new voltage clamp method for Ranvier nodes. *Pflügers Archiv* **309**, 116–192.

NONNER, W. (1979). Effects of *Leiurus* scorpion venom on the 'gating' current in myelinated nerve. *Advances in Cytopharmacology* **3**, 345–352.

ROCHAT, H., BERNARD, P. & COURAUD, F. (1979). Scorpion toxins: chemistry and mode of action. *Advances in Cytopharmacology* **3**, 325–334.

SCHMIDTMAYER, J. (1985). Behaviour of chemically modified sodium channels in frog nerve supports a three-state model of inactivation. *Pflügers Archiv* **404**, 21–28.

SCHMIDTMAYER, J., STOYE-HERZOG, M. & ULBRICHT, W. (1982). Rate of action of *Anemonia sulcata* toxin II on sodium channels in myelinated nerve fibres. *Pflügers Archiv* **394**, 313–319.

SWENSON, R. P. & ARMSTRONG, C. M. (1981). K^+ channels close more slowly in the presence of external K^+ and Rb^+. *Nature* **291**, 427.

ULBRICHT, W. & SCHMIDTMAYER, J. (1981). Modification of sodium channels in myelinated nerve by *Anemonia sulcata* toxin II. *Journal de physiologie* **77**, 1103–1111.

WANG, G. K. & STRICHARTZ, G. (1984). Rapid voltage-dependent binding of α-scorpion toxins to Na^+ channels *Neuroscience Abstracts* **10**, 864.

WANG, G. K. & STRICHARTZ, G. (1985). Kinetic analysis of the action of *Leiurus* scorpion α-toxin on ionic currents in myelinated nerve. *Journal of General Physiology* **86**, 739–762.

WOODHULL, A. M. (1973). Ionic blockage of sodium channels. *Journal of General Physiology* **61**, 687–708.

YAMAMOTO, D., YEH, J. Z. & NARAHASHI, T. (1985). Interactions of permeant cations with sodium channels of squid axon membranes. *Biophysical Journal* **48**, 361–368.